

# LATEST FINDING ON FUNDAMENTAL PROPERTIES: CEMENTITE

Pravrati Taank<sup>1</sup>, Tassawur Jahan<sup>2</sup>, Akshay Jain<sup>3</sup>

<sup>1,2</sup> Department of Basic and Applied Sciences, Modi Institute of Management and Technology, Kota (India)

<sup>3</sup> Former, Assistant professor in RTU (2014-15), Kota (India)

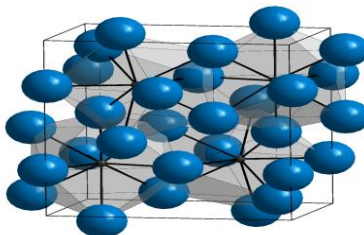
## ABSTRACT

The fundamental properties of cementite ( $Fe_3C$ ) in the literatures have been reviewed. The nonisotropic crystal structure of cementite and its effect on the mechanical and physical properties are presented. The effect of annealing temperature and alloying content on the lattice parameters has been summarized. The thermodynamic of cementite such as specific heat, formation free energy are discussed. The engineering importances and thermodynamical stability of alloyed cementite are discussed. Finally the mechanical properties, thermal properties and magnetic properties of cementite have been presented.

**Key Words:** Cementite, Orthorhombic, Intermetallic Compound, Nonisotropic Crystal

## I INTRODUCTION

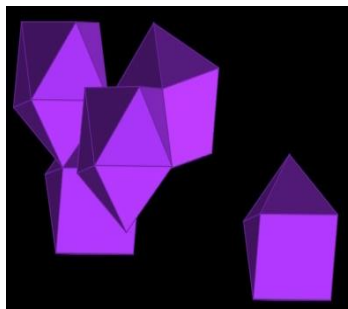
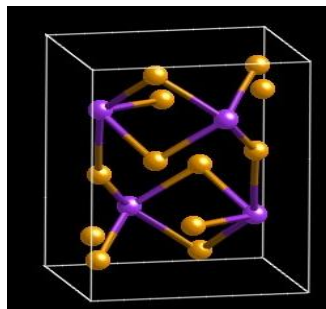
Cementite, also known as iron carbide, an intermetallic compound of iron and carbon, more precisely an intermediate transition metal carbide with the formula  $Fe_3C$ . By weight, it is 6.67% carbon and 93.3% iron. It has an orthorhombic crystal structure. It is a hard, brittle material, normally classified as a ceramic in its pure form, and is a frequent found and important constituent in ferrous metallurgy. While iron carbide is present in most steels and cast irons, it is produced as a raw material in the Iron Carbide process, which belongs to the family of alternative iron making technologies. It has density  $7.69 \text{ g/cm}^3$ , melting point  $1837^\circ\text{C}$  and it is insoluble in water. Cementite has an orthorhombic lattice with approximate parameters 0.45165, 0.50837 and 0.67297 nm. There are twelve iron atoms and four carbon atoms per unit cell, corresponding to the formula  $Fe_3C$ .



Orthorhombic  $Fe_3C$ . Iron atoms are blue. Cementite changes from ferromagnetic to paramagnetic at its Curie temperature of approximately 480 K.<sup>[4]</sup> A natural iron carbide (containing minor amounts of nickel and cobalt)

occurs in iron meteorites and is called cohenite after the German mineralogist Emil Cohen, who first described

it.<sup>[5]</sup> As carbon is one of the possible minor light alloy components of metallic planetary cores, the high-pressure/high-temperature properties of cementite ( $Fe_3C$ ) as a simple proxy for cohenite are studied experimentally.



This figure shows the coordination polyhedron, in which eight iron atoms surround a carbon atom. The polyhedron consists of a square base and eight triangles.

**II The fundamental properties of cementite are we are discussing here -**

1. Mechanical properties
2. Magnetic properties
3. Thermodynamic properties

**Table-1 Fundamental Properties of Cementite**

Characteristics	Values	References
Crystal structure	Orthorhombic, Space group : Pbnm	9-12
Lattice constant	a = 4.525 Å, b = 5.090 Å, c = 6.743 Å	13
Unit cell	Volume 155.3 Å <sup>3</sup> Fe 12, C 4 atoms	13
Weight	179.56 g/mol (= 55.85×3+12.01) 44.89 g/g·atom	
Molar Volume	23.4 cc/mol (20°C)	
Density	7.68 g/cm <sup>3</sup> (20°C)	
Melting point	1252 °C	3
Formation energy	$\Delta G = 19.97 \text{ kJ/mol}$ , $\Delta H = 25.04 \text{ kJ/mol}$ $3Fe(l) + C(\text{graph}) \rightarrow Fe_3C$ $\Delta S = 105 \text{ J/mol}\cdot\text{deg}$	28
Specific heat	$C_p = 90.17 + 63.01 \times 10^{-3}T \text{ J/mol}$ (273-463K) $C_p = 113.0 + 61.1 \times 10^{-3}T \text{ J/mol}$ (463K-1473K)	29
Volume change due to decomposition	+13.8 % (20°C) , +12.8% (1000°C) (7.09×3+5.30-23.4) / 23.4 (20°C) (7.30×3+5.40-24.2) / 24.2 (1000°C)	
Young's modulus	140 ~ 300GPa (polycrystal) 180~190 GPa	30-35 13
Hardness	10~13 GPa	22, 34, 36,63
Thermal expansion coefficient	$16 \sim 17 \times 10^{-6}$ (300~500°C)	24, 35, 37
Electrical resistivity	$100 \mu \Omega \cdot \text{cm}$ (20°C)	38, 39,65
Curie point	220°C (600°C annealed)	13
Saturation magnetization	15~16 T (20°C)	40, 41

This figure shows the crystal structure of cementite. The purple atoms represent carbon. Each carbon atom is surrounded by eight iron atoms. Each iron atom is connected to three carbon atoms.

### 2.1 Mechanical properties

Cementite is one of the most important phases in steels, which plays a critical role in the mechanical properties of steels. However, the deformation behavior of cementite has not been understood well. The present study aims to study the deformation behavior of cementite in steels and fine grained bulk cementite in detail and try to find out the relation between the plastic deformation and dissolution of cementite lamellae and superplastic deformation of fine grained cementite.

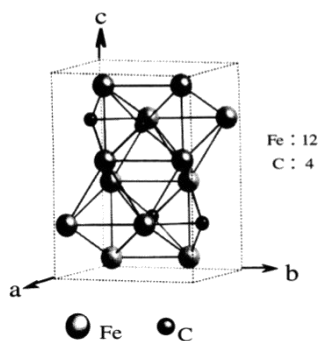


Fig.1. Unit cell of cementite

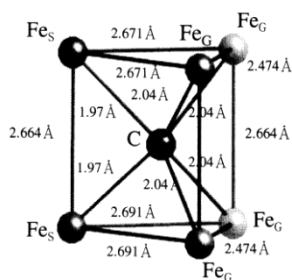


Fig. 2. Local structure of cementite around carbon atom, consisting of a trigonal prism composed of six Fe atoms and one carbon atom. Fe<sub>G</sub> denotes Fe atom at general site and Fe<sub>S</sub> denotes the one at special site.

Structural, elastic, and thermal properties of cementite (Fe<sub>3</sub>C) can be studied using a modified embedded atom method (MEAM) potential for iron-carbon (Fe-C) alloys. Previously developed Fe and C single-element potentials can be used to develop a Fe-C alloy

MEAM potential, using a statistics-based optimization scheme to reproduce structural and elastic properties of cementite, the interstitial energies of C in bcc Fe, and heat of formation of Fe-C alloys in L<sub>12</sub> and B<sub>1</sub> structures. The stability of cementite can be investigated by molecular dynamics simulations at high temperatures. The nine single-crystal elastic constants for cementite can be obtained by computing total energies for strained cells. Polycrystalline elastic moduli for cementite can be calculated from the single-crystal elastic constants of cementite.



## 2.2 Magnetic Properties

First theoretical considerations and calculations of the critical size of magnetic particle (typically few nanometers), that is the size below which the most energetically favorable magnetic state is a single domain state, were carried out by Charles Kittel in 1946. Superparamagnetism is the phenomenon by which the system containing single domain magnetic nanoparticles, dispersed in a nonmagnetic matrix, may exhibit at temperatures above the so-called blocking temperature  $T_B$ , a behavior similar to that of a paramagnetic material. At a temperature higher than the blocking temperature, a stable bulk magnetization cannot be established because of thermal fluctuations acting on each particle in a system, and so the bulk material exhibits superparamagnetism. At temperatures below  $T_B$ , thermal fluctuations cannot overcome the energy barrier connected with the magneto-crystalline anisotropy energy, and then magnetic moments of particles are confined in random directions, lying along easy axis of magnetization and cannot change their directions spontaneously from one easy direction to the other. The first model of monodispersed, non interacting, single domain magnetic particles with uniaxial anisotropy, embedded in a nonmagnetic matrix was proposed by Stoner and Wohlfarth. The thermal relaxation of magnetic nanoparticles is excellently described by the Arrhenius–Néel formula:

$$t_{rel} = t_0 \exp\left(\frac{E_A}{K_B T}\right)$$

where  $t_{rel}$  is the relaxation time of the particle magnetic moment,  $E_A$  is the anisotropy energy barrier,  $t_0$  is the characteristic relaxation time, barrier, ranging typically from  $10^{-11}$  to  $10^{-9}$  s. In the absence of external magnetic field, the anisotropy barrier  $E_A$  is proportional to the particle volume,  $V$ , and can be expressed as

$E_A = KV\sin^2 \alpha$ , where  $K$  is the effective magnetic anisotropy constant and  $\alpha$  is the angle between magnetic moment of the particle and its easy magnetization direction. In the recent decade, great attention has been focused on magnetic nanoparticles because of their unique physical properties and also because of the possibility of their practical application in medicine and biotechnology (e.g., hyperthermia, targeted drug delivery, contrast agents in MRI) as well as in catalysis, magnetic separation, gas sensors and many others. The aim of the present work was to investigate structural characteristics and magnetic properties of nanoparticle agglomerates of iron carbide ( $Fe_3C$ ) embedded in a carbon matrix. 2. Preparation of samples and shape characterization.

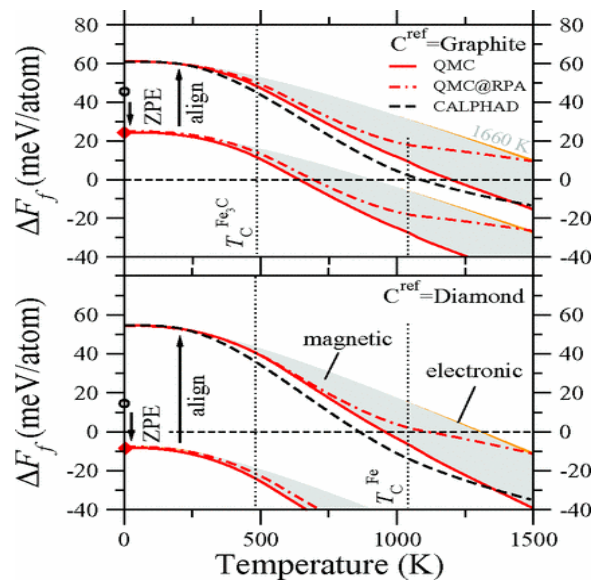
## 2.3 Thermodynamical Property

In the present work, the thermodynamic properties of cementite are reevaluated and Gibbs energy functions valid from 0 K upwards presented. At high temperature (1000 K and above), the Gibbs energy is practically unchanged compared to previous evaluations. The energy of formation at 0 K was also calculated using density functional theory. This energy of formation (+8 kJ/mol at 0 K) is in reasonable agreement with the present thermodynamic evaluation (+23.5 kJ/mol at 0 K and +27.0 kJ/mol at 298.15 K) and with a solution calorimetric measurement of the enthalpy of formation (+18.8 kJ/mol at 298.15 K)



Table-2 Thermodynamic properties of cementite

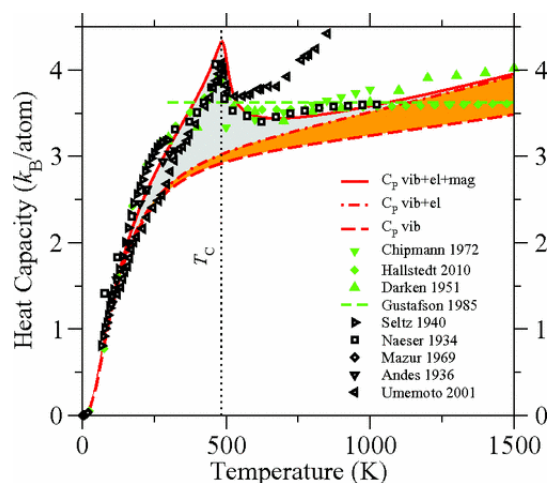
T. K	C <sub>p</sub> J/K·mol	H <sub>T</sub> -H <sub>st</sub> kJ/mol	S <sub>T</sub> -S <sub>st</sub> J/mol·K	S <sup>0</sup> J/mol·K	3Fe(α) + C(gr) = Fe <sub>3</sub> C		
					ΔG <sup>0</sup> <sub>T</sub> kJ/mol	ΔH <sup>0</sup> <sub>T</sub> kJ/mol	ΔS <sup>0</sup> <sub>T</sub> J/mol·K
298.15	106.2	0	0	104.5	19.74	25.02	17.01
400	116.7	11.33	32.60	137.10	17.87	27.31	23.62
450	125.3	17.31	46.86	151.36	16.51	28.43	26.50
480	128.4	21.12	55.05	159.55			
500	110.8	23.51	59.94	164.44	15.12	29.61	28.97
600	113.7	34.73	80.38	184.88	12.19	30.00	29.68
700	116.6	46.25	98.15	202.65	9.25	29.77	29.30
800	119.5	58.06	113.91	218.41	6.37	28.81	28.05
850	121.0	64.07	121.18	225.68	4.98	27.97	27.04
900	122.5	70.16	128.12	232.62	3.70	26.80	25.67
950	123.9	76.32	135.18	239.26	2.45	25.16	23.91
1000	125.4	82.55	141.20	245.70	1.25	22.78	21.52



Upper figure shows the theoretically free energy of formation of cementite from the pure compounds (bcc Fe and graphite) at zero pressure as a function of temperature and including zero-point vibrations. But the lower figure shows that experimentally when assuming the diamond phase (where van der Waals interactions are absent and which is used only as a benchmark) are shown in the lower figure. The open black circles show the T=0 K data without zero-point vibrations. The black dashed curve, referred to as calphad, gives the thermodynamic assessment (for α- Fe, Fe<sub>3</sub>C, graphite) and the thermocalc program with the sgte unary database(diamond), based on experimental data. For an easier comparison of the temperature dependence the present theoretical curves aligned to

the calphad value at  $T=200$  K are also shown. The calculated electronic and magnetic contributions to the free energy are shown in shaded orange and gray correspondingly.

Calculated heat capacity (CP at  $p=0$ ) of cementite as a function of temperature T in comparison with available experimental data (open symbols) and thermodynamic assessments (filled symbols). The calculated electronic and magnetic contributions to the heat capacity are shown in shaded orange and gray correspondingly



### III CONCLUSION

Different different properties of cementite have discussed here. Cementite shows different different behavior at different places. So that we can use it with different alloys in the experiments. By this review one may get information about the properties of cementite. This review may help the future researcher to devise a concrete strategy for evaluating different properties of cementite. However further study is needed to reveal all the aspects of it.

### REFERENCES

1. Didukh P., Nedelko O., Ślawska-Waniewska A., J. Magn. Magn. Mater., 242 (2002), 1077.
2. Yoshida J., Kobayashi T., J. Magn. Magn. Mater., 194 (1999), 176.
3. Panatarotto D., Prtidos C.D., Hoebeke J., Brown F., Kramer E., Briand J.P., Muller S.,
4. Prato M., Bianco A., Chem. Biol., 10 (2003), 961.
5. Weissleder R., Elizondo G., Wittenburg J., Rabito C.A., Bengel H.H., Josephson L., Radiol., 175 (1990), 489.
6. Narkiewicz U., Kucharewicz I., Arabczyk W., Lenart S., Mater. Sci.-Poland, 23 (2005), 939. Narkiewicz U., Kucharewicz I., Arabczyk W., Lenart S., Mater. Sci.-Poland, 23 (2005), 939.
7. Jin Lu Lu, Hong Yuan Deng, Huei Li Huan, J. Magn. Magn. Mater., 209 (2000), 37.
8. Candela G.A., Haines R.A., Appl. Phys. Lett., 34 (1979), 868.
9. Vagn F. Buchwald, Handbook Of Iron Meteorites, University Of California Press 1975.



10. Jump Up<sup>^</sup> Gunnar Hägg, *Z. Krist.*, Vol. 89, P 92-94, 1934.
11. Ślawska-Waniewska A., Gutowski M., Lachowicz H.K., Kulik T., Matyja H., *Phys. Rev. B*, 46 (1992), 14594.
12. Kittel C., *Phys. Rev.*, 70 (1946), 965.
13. Stoner E.C., Wohlfarth E.P., *Ieee Trans. Magn.*, 27 (1991), 3475.
14. Néel L., *Compt Rend. (Paris)*, 228 (1949), 604.